Arch. Metall. Mater. **66** (2021), 4, 1029-1032

DOI: 10.24425/amm.2021.136419

JEONG-HAN LEE[1], IK-HYUN-OH[1], HYUN-KUK-PARK[1*]

# EFFECTS OF TRANSITION METAL CARBIDES ON MICROSTRUCTURE AND MECHANICAL PROPERTIES OF ULTRAFINE TUNGSTEN CARBIDE VIA SPARK PLASMA SINTERING

WC-Co cemented carbides were consolidated using spark plasma sintering in the temperature 1400°C with transition metal carbides addition. The densification depended on exponentially as a function of sintering exponent. Moreover, the secondary (M, W) $C_x$ phases were formed at the grain boundaries of WC basal facet. Corresponded, to increase the basal facets lead to the plastic deformation and oriented grain growth. A higher hardness was correlated with their grain size and lattice strain. We suggest that this is due to the formation energy of (M, W)$C_x$ attributed to inhibit the grain growth and separates the WC/Co interface.

*Keywords:* WC cemented carbide, transition metal carbide, spark plasma sintering, grain growth inhibitor, hardness

## 1. Introduction

Carbides of transition metals are used widely in manufacturing structures and tool materials that can operate at high temperatures, in aggressive media, and heavy loads [1]. However, using WC-cemented carbide as a cutting tool material exhibits its vulnerable properties such as brittleness and sinterability. Therefore, Co is added between the WC particles as a binder, which contributes to wettability and ductility. The Co decreases the wear and corrosion resistance of the WC matrix, which is caused by abnormal grain growth of the cemented carbide and electrochemical elution of Co [2].

Methods such as rapid sintering (spark plasma sintering; SPS) and adding of inhibitors can improve the aforementioned properties that control the finer grain size in the WC-cemented carbide to be less than 0.5 μm. Thus, the mechanism of grain growth inhibition was essential for improving the mechanical properties of the WC-cemented carbide, in which the transition metal carbides (MCs) (such as TiC, VC, $Cr_3C_2$, ZrC, TaC, and NbC) act as inhibitors by forming a secondary mixed cubic carbide phase, that is, (M, W)$C_x$. The (M, W)$C_x$ stability is correlated with the mechanical properties of the cemented carbide, wherein the influence of the (M, W)$C_x$ on the interactions for crack-microstructure is effected of GGI on the interface structures of the WC/Co [3].

According to previous literature, the effect of adding MCs can be classified as follows: (i) TiC increase the wear resistance by diffusive wear and chemical interaction [4]. (ii) TaC and ZrC are hardened to interfere with plastic deformation, whereas high hardness is observed at high temperatures [4]. (iii) NbC reduces the oxidation rate via the passivation effect [5]. (iv) VC and $Cr_3Cr_2$ are hardened to inhibit grain growth by high solubility in the binder phase [5].

This study designs strengthened WC-Co-based hard materials containing MCs via SPS. Herein, the WC-6Co-2.5MCs sintered compacts are consolidated during rapid densification with the inhibition of particle growth. Notably, the structural evolution, sintering behavior, microstructure, and mechanical properties were investigated according to the effect of GGIs

## 2. Experimental

WC (≤0.5 μm, >99.9%, Taegutac Ltd.), Co (≤10.0 μm, >99.8%, Alfa Aesar), $Cr_3C_2$ (≤10.0 μm, >99.5%, Alfa Aesar), NbC (≤10.0 μm, >99.0%, Kojundo Chemical), TaC (≤44.0 μm, >99.5%, Alfa Aesar), TiC (≤5.0 μm, >99.5%, Alfa Aesar), VC (≤2.0 μm, >99.5%, Alfa Aesar), and ZrC (≤10.0 μm, >99.5%, Alfa Aesar) powders were used as raw materials. These powders were synthesized via horizontal ball milling with $ZrO_2$ balls at

[1] KOREA INSTITUTE OF INDUSTRIAL TECHNOLOGY, SMART MOBILITY MATERIALS AND COMPONENTS R&D GROUP, 6, CHEOMDAN-GWAGIRO 208-GIL, BUK-GU, GWANG-JU, 61012, KOREA

* Corresponding author: hk-park@kitech.re.kr

a ball-to-powder ratio of 10:1. The powder mixture was milled for 12 h in ethanol media at 250 rpm. The nominal compositions of the powders were WC-6Co-2.5MCs (wt.%).

The milled powders were consolidated via SPS (SPS 9.40 MK-III, Sumitomo Heavy Industries) at a sintering temperature 1400°C, heating rate of 60°C/min, and under a pressure of 60 MPa. The sintering behavior during densification and consolidation was investigated according to the macroscopic shrinkage strain in Eq. (1).

$$\varepsilon_s^m = \left(\frac{\Delta L}{L_0}\right)^m = -\left(\frac{X}{2D}\right)^2,\ \rho_S = \frac{\rho_G}{\left(1-\frac{\Delta L}{L_0}\right)^3} \quad (1)$$

Where, $\varepsilon_s$ is the shrinkage strain, $m$ is the sintering exponent, $\Delta L$ is the change in shrinkage displacement, $L_0$ is the original length of the green body, $\rho_S$ is the sintered relative density, $\rho_G$ is the density of the green body, and (X/2D) is the neck-to-particle diameter ratio of the sintered particles.

Structural evolution of the milled powders and sintered compacts was characterized via X-ray diffraction (XRD, PIXCEL 1D DETECTOR, Panalytical) with CuKα radiation ($\lambda = 0.154$ nm). The average crystallite size and microstrain were calculated using a Willamson-Hall plot in Eq. (2).

$$D = \frac{k\lambda}{\beta_{hkl}\cos\theta},\ \varepsilon = \frac{\beta_{hkl}}{4\tan\theta} \quad (2)$$

Where, $D$ is the crystallite size, $k$ is Scherrer constant (0.9) with shape factor, and $\lambda$ is the wavelength of CuKα radiation. Instrumental broadening is expressed as $\beta_{hkl}$ of the corrected value derived using the micro strain ($\varepsilon$). In addition, the WC grain size was obtained from Image-Pro software (6.0 ver., Media Cybernetics) from the FE-SEM images by measuring the linear intercept length.

The microstructure of the sintered compacts was observed via scanning electron microscopy (SEM, JSM-7001F, JEOL), and their mechanical properties were measured using a Vickers hardness tester (HMV-G, Shimadzu) with a load of 20 kg·f applied for 15s. The hardness is calculated with the Eq. (3).

$$H_v = \frac{kP}{d^2} \quad (3)$$

Where, $k$ is a constant ($= 1.89 \times 10^5$) depending on the indenter geometry and on the units, $P$ is the applied force (in N) and $d$ the diagonal length of the indentation.

In addition, the fracture toughness ($K_{IC}$) value obtained by the Antis formula [6] is expressed using Eq. (4).

$$K_{IC} = 0.016\left(\frac{E}{Hv}\right)^{1/2} P/C^{3/2} \quad (4)$$

Where, $E$ is the elastic modulus, $H_v$ is the hardness, $P$ is the applied load, and $C$ is the length of crack propagation.

## 3. Results and discussion

XRD patterns of powders and sintered compacts were showed Figure 1. The (M, W)$C_x$ phases were observed at the basal facets of the cemented carbide, that is, the (001) plane. The increase in basal facets could lead to the plastic deformation of the cemented carbide [1], which causes preferentially oriented grain growth. In the specimen containing the $Cr_3C2$ (Fig. 1(b)-v) and NbC (Fig. 1(b)-vi), the peak intensity of the basal facets was relatively high; therefore, the brittle to ductile transition in the cemented carbide [7] was increased. Contrarily, the precipitation of free carbon (graphite) is shown in Fig. 1(b)-iii, to which VC was added. This is because the W and carbon atoms of (V, W)$C_x$ at the interface between WC/Co hardly diffused into the Co intergranular [8] owing to the difference in carbon activity. Consequently, (M, W)$C_x$ could cause grain refinement by decreasing the interfacial resistance along with the instability of the interface.

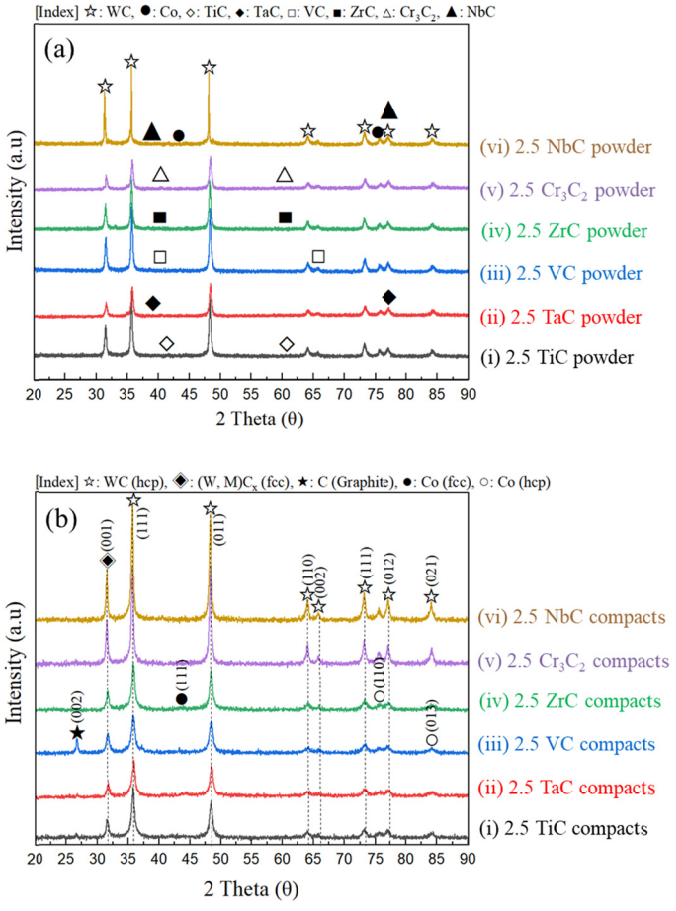


Fig. 1. XRD patterns of WC-6Co-2.5MCs sintered-compacts: (a) 2.5TiC, (b) 2.5TaC, (c) 2.5VC, (d) 2.5ZrC, (d) $Cr_3C_2$, and (e) 2.5NbC

The densification profile and sintering kinetics of sintered compacts are shown in Figure 2. The relative densities of all compacts were consolidated to be above 99.0% with the measured macroscopic shrinkage profile, that is, 6Co: 100.0%, 2.5TiC: 100%, 2.5$Cr_3C_2$: 99.8%, 2.5VC: 99.6%, 2.5TaC: 99.3%, 2.5NbC: 99.1%, and 2.5ZrC: 99.0%. The high densification was

confirmed by boosting the atomic diffusion of the WC particles by Joule heat at the particle to particle contact point by pulsed DC current during the rapid sintering. In addition, the densification strain for the sintering exponent for the WC-6Co-2.5MCs in the temperature range (900~1200)°C, where rapid shrinkage proceeds, is shown in Fig. 2(b). That is, the high $\varepsilon_s$ increases exponentially as a function of $m$.

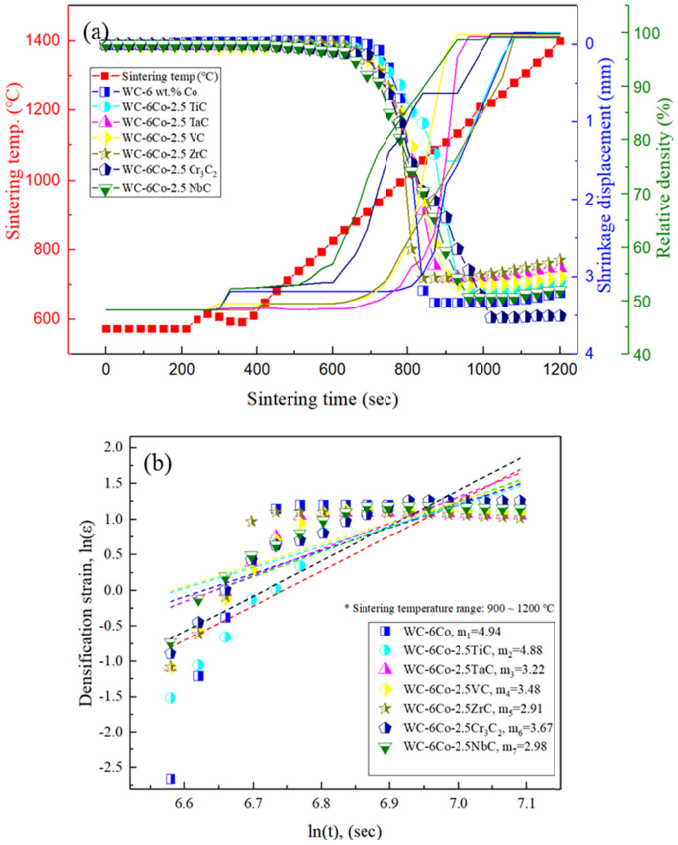


Fig. 2. Schematic representation of SPS process with WC-6Co-2.5MCs sintered-compacts: (a) shrinkage displacement and relative density profile and (b) densification strain-sintering time curve in shrinkage stage, i.e., at the temperature range of 900~1200°C

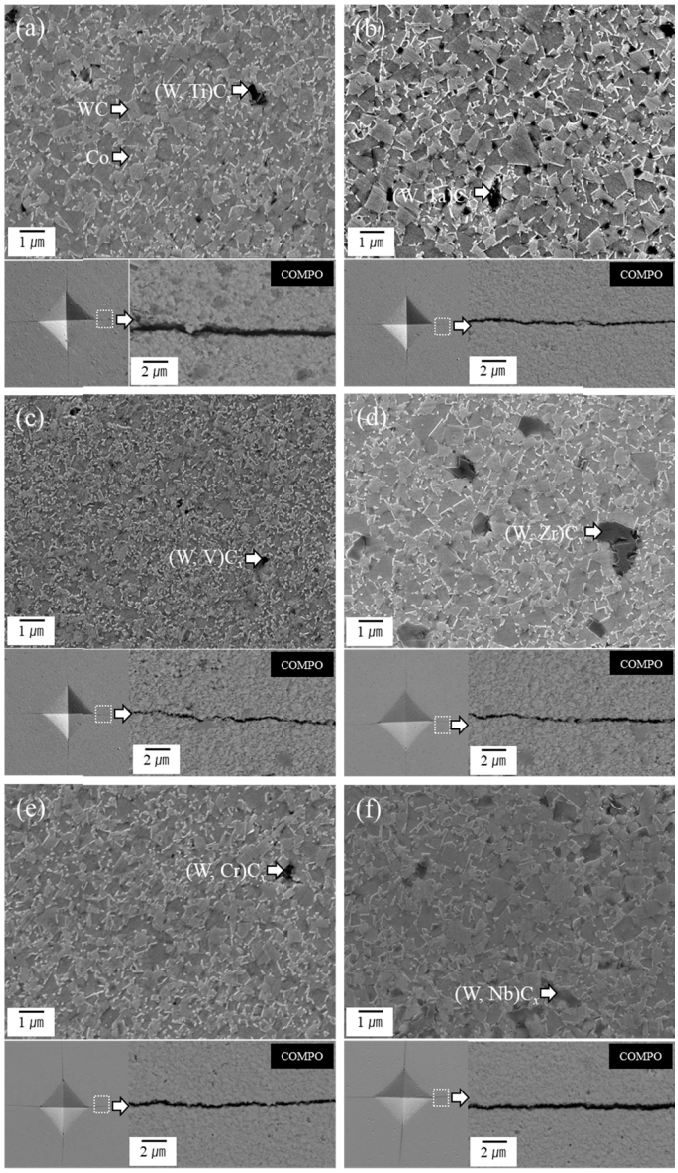


* Gray: WC, Light gray: Co, Black: (W, M)$C_x$

Fig. 3. Microstructures of WC-6Co-2.5MCs sintered-compacts with their crack propagations: (i) 2.5TiC, (ii) 2.5TaC, (iii) 2.5VC, (iv) 2.5ZrC, (v) 2.5$Cr_3C_2$, and (vi) 2.5NbC

Microstructures of sintered compacts with their crack propagation and indentation are shown in Figure 3. They consists of the WC-6Co-2.5MCs in angular WC grains (gray color) and Co-binder (light gray), which are embedded in the rounded (M, W)$C_x$ phase (light gray). The high concentration of (M, W)$C_x$ in the TaC (Fig. 3(b), −2.426 eV) and the $Cr_3C2$ (Fig. 3(e), −2.778 eV) was attributed to their formation energies [9] of the cubic carbides. For instance, $WC_x$: −2.167 eV, (W, V)$C_x$: −1.576 eV, (W, Ti)$C_x$: 0.282 eV, (W, Nb)$C_x$: −1.481 eV, and (W, Zr)$C_x$: −1.528 eV. Moreover, owing to the low stability in the Co-binder at high carbon activities, they cause instability of the interface, and then segregate as agglomerates rather than diffusing to grain boundaries. However, the stabilized cubic carbides (Fig. 3(a) and 3(c)) not only inhibits the growth of the WC grain but also separates the bonding of the WC/Co interface, which causes a decrease in the resistance against intergranular fracture [9].

Mechanical and structural properties of the WC-6Co-2.5MCs sintered compacts are summarized in Table 1. The average hardness increased from 17.2±0.3 to 22.3±0.3 GPa, whereas the $K_{IC}$ decreased from 12.3±0.4 to 4.3±0.5 MPa·$m^{1/2}$. The effect of inhibiting grain growth was most effective when the VC was added (0.80 to 0.52 μm) with a highly internal strain ($\varepsilon$ = 0.48) of the lattice. That is, the decrease in the lattice constant (2.837 to 2.821 Å) could be attributed to a series of solid solution strengthening. Therefore, an adequate phase constitution between the carbon activity and stability of the cubic carbide can lead to both strengthening effects ($H$ and $K_{IC}$). It can be observed in the properties of the WC-6Co-2.5TaC, that is, 20.1±0.2 GPa and 6.4±0.4 MPa·$m^{1/2}$.

TABLE 1

Comparison of the mechanical and structural properties of the WC-6Co and the WC-6Co-2.5MCs sintered compacts

| WC-6Co-2.5MCs | Properties | | | | | | |
|---|---|---|---|---|---|---|---|
| | Vickers hardness (GPa) | Elastic modulus (GPa) | Fracture toughness ($MPa \cdot m^{1/2}$) | Average crystallite size (nm) | Average grain size (μm) | Lattice constant (W,M)Cx (Å) | Mircostrain (%) |
| WC-6Co | 17.2±0.3 | 666.8 | 12.3±0.4 | 44.8 | 0.80 | 2.837 | 0.18 |
| WC-6Co-2.5$Cr_3C_2$ | 16.2±0.1 | 655.0 | 10.2±0.3 | 33.0 | 0.71 | 2.837 | 0.25 |
| WC-6Co-2.5NbC | 18.1±0.1 | 656.2 | 8.1±0.3 | 39.2 | 0.74 | 2.838 | 0.24 |
| WC-6Co-2.5ZrC | 18.9±0.3 | 655.8 | 6.8±0.5 | 28.6 | 0.69 | 2.823 | 0.34 |
| WC-6Co-2.5TiC | 19.6±0.3 | 655.4 | 4.8±0.5 | 25.7 | 0.64 | 2.833 | 0.36 |
| WC-6Co-2.5TaC | 20.1±0.2 | 653.7 | 6.4±0.4 | 24.4 | 0.58 | 2.817 | 0.39 |
| WC-6Co-2.5VC | 22.3±0.3 | 655.1 | 4.3±0.5 | 17.8 | 0.52 | 2.821 | 0.48 |

## 4. Conclusions

Effect of adding MCs that cause the grain refining behavior of the WC-Co cemented carbide was discussed. SPS enhanced the sintering kinetics and maintained the fine grains. Phase constitution and microstructure distribution of the (M, W)$C_x$ cubic carbides were dominated by the behavior of the WC basal facet and carbon activity on the Co interface, which was similar to their formation energy. Mechanical properties were characterized by considering the grain size and lattice strain, which exhibited the highest hardness value (22.3±0.3 GPa) on adding by the VC due to the solid solution strengthening.

**Acknowledgments**

This study has been conducted with the support of the Korea Institute of Industrial Technology as "Production technology commercialization project" (KITECH EH-21-020).

## REFERENCES

[1] A.I. Gusev, A.A. Remple, A.J. Magerl, Disorder and order in strongly non-stoichiometric compounds: transition metal carbides, nitrides and oxide. Berlin: Springer; 607 (2001).

[2] T.A. Fabijanic, M. Kurtela, I. Skrinjaric, J. Potschke, M. Mayer, Metals **10**, 224 (2020).

[3] X. Liu, X. Song, H. Wang, X. Liu, F. Tang, H. Lu, Acta Materialia **149**, 164-178 (2018).

[4] H.O. Andren, Microstructures of cemented carbides, Mater. Des. **22**, 491-498 (2001).

[5] C. Barbatti, J. Garcia, P. Brito, A.R. Pyzalla, Int. J. Refract. Met. Hard Mater. **27**, 768-776 (2009).

[6] G.R. Antis, P. Chantikul, B.R. Lawn, D.B. Marshall, J. Am. Ceram. Soc. **64** (9), 533-538 (1981).

[7] Y.V. Milman, J. Superhard Mater. **36**, 65-81 (2014).

[8] M. Christensen, G. Wahnstrom, Acta Materialia **52** (8), 2199-2207 (2004).

[9] Y. Peng, H. Miao, Z. Peng, Int. J. Refract. Met. Hard Mater. **39**, 78-89 (2013).